



The anatomical classification of AICA/PICA branching and configurations in the cerebellopontine angle area on 3D-drive thin slice T2WI MRI

Nobukata Kazawa^{a,*}, Kaori Togashi^a, Juichi Ito^b

^aDepartment of Radiology, Kyoto University Hospital, Kyoto-City, Kyoto 606-8507, Japan

^bDepartment of Otolaryngology, Kyoto University Hospital, Kyoto-City, Kyoto 606-8507, Japan

Received 13 August 2011; accepted 21 November 2011

Abstract

Background: With the technical advance of magnetic resonance imaging (MRI), we have been able to observe not only the small cranial nerves arising from the brain stem but also the branches of vertebrobasilar artery in the cerebellopontine angle (CPA) cistern. **Purpose:** The purpose was to demonstrate the courses and configurations of the anterior inferior cerebellar artery (AICA) or posterior inferior cerebellar artery (PICA) branch including the internal auditory artery in the CPA cistern and evaluate the relationship between the facial–vestibulocochlear (VIIth–VIIIth) nerves and AICA/PICA on high-resolution, thin-slice, three-dimensional T2-weighted MRI using driven equilibrium pulse. **Material and methods:** Thirty-three men and 27 women aged 8–85 years old with sensory hearing loss or vertigo, and/or tinnitus were evaluated by thin-slice (0.75 mm) T2-weighted MRI. ~~Forty sides of ears of 30 subjects (17 men, 13 women) had normal auditory function on both sides (10 subjects) or only one side of auditory symptoms (30 subjects).~~ **Results:** Thin-slice T2WI drive MRI revealed several variations of the AICA/PICA coursing, such as a loop formation ($n=33$, 49 sides) or the IAC extension ($n=20$, 30 sides). Contact with the vestibulocochlear nerve was seen in 31.7% of subjects ($n=19$). The AICA/PICA branching and shape patterns relative to the CPA and IAC were classified into four major types: type 1A, nonloop AICA/PICA in the CPA cistern; type 1 B, nonloop AICA/PICA (internal auditory artery) entering the IAC; type 2A, loop-type AICA/PICA in the CPA cistern; and type 2B, loop-type AICA/PICA entering the IAC. **Conclusion:** There were statistically significant associations between types 1A and 2A ($P<.01$) regarding the existence of any auditory 3 symptoms. The results of our study suggest that this classification is simple and very useful for the elucidation of the mechanism of auditory symptoms and deciding the therapeutic strategies.

© 2012 Elsevier Inc. All rights reserved.

Keywords: Head and neck; MR imaging; Anatomical topics; 3D-drive-T2WI, Anterior inferior cerebellar artery (AICA), Posterior inferior cerebellar artery (PICA), Vestibulocochlear (VIIIth) cranial nerve, Nerve–vascular compression syndrome

For the evaluation of the temporal bone including the internal auditory canal (IAC) and the cerebellopontine angle (CPA) area, magnetic resonance imaging (MRI) has been commonly used in patients with auditory symptoms [1–3]. Besides surgical tumor resection, therapeutic option such as stereotactic radiation therapy for the acoustic tumor has been introduced into practice [4] recently. Therefore, its early detection and the correct diagnosis are very important. Usually, the anterior inferior cerebellar artery (AICA)

courses backward around the pons three-dimensionally toward CPA cistern to supply the inferolateral pons, middle cerebellar peduncle, flocculus, and anterior margins of cerebellar hemispheres. In some cases, they anastomose with the terminal branch of the posterior inferior cerebral artery (PICA) [5,6]. The PICA runs beneath the cerebellum and supplies the posteroinferior cerebellum, tonsil, inferior vermis, choroid plexus of the fourth ventricle, and posterolateral medulla. These vessels usually arise from the vertebral or basilar artery asymmetrically. There, perfusion areas are reciprocal. ~~At some time,~~ AICA or PICA is absent bilaterally [7,8]. The internal auditory artery (IAA) supplying the inner ear was hard to be observed on the conventional angiography. There have been scant radiological reports

* Corresponding author. Department of Radiology, Kyoto Yoshikawa Hospital, Shogoin Kawaharama chi 54 Sakyo, Kyoto-City, Kyoto 606-8507, Japan. Tel.: +81 75 761 03 16; fax: +81 75 771 0528.

E-mail address: nk1207@kuhp.kyoto-u.ac.jp (N. Kazawa).

describing the precise course and branching patterns of these vessels in humans [5–7]. For further detailed analysis of the inner ear including the running course of the IAA, AICA, and/or PICA, 55 patients were examined on thin-slice T2WI images using driven equilibrium pulse sequence. Occasionally, they ran between the facial and vestibulocochlear nerve and contacted with them. In some previous reports, the precipitation of the auditory nerve symptoms such as tinnitus, sensorineural hearing loss, and vertigo was caused by such loops (nerve vascular compression syndrome). It is difficult to discriminate them with certainty both on the conventional T2WI (slice thickness 4–5 mm) and on the thin-slice images. Unusual manifestations such as distal AICA (IAA) entering the IAC in contact with the facial or vestibular nerve were presented in our study (Fig. 4). Our purpose was to demonstrate the inner ear auditory artery and evaluate the relationship between the facial–vestibular cochlear (seventh–eighth) nerves and the branches of AICA/PICA on high-resolution thin-sliced three-dimensional (3D) T2-weighted MRI using driven equilibrium pulse sequence. To the best of our knowledge, this is the first study describing the coursing patterns of the AICA or PICA relative to the CPA and IAC on thin-slice T2WI MRI.

1. Material and methods

From September 2006 to August 2011, a total of 55 consecutive patients (30 men and 25 women aged 8–85 years old; mean age 53.4 years old) with sensory hearing loss or vertigo, dizziness, and/or tinnitus were examined with 1.5-T Intera Achieva MRI scanner with sense coil (Philips Medical System, Best, the Netherlands). Five subjects (three men, two women) without any auditory symptoms were also included in this study. On each subject, the informed consent was obtained. Our institutional ethics committee also approved the purpose and protocol of this study. For the high-resolution MR images, 3D fast spin echo T2WI with drive equilibrium pulse was used; the scanning parameters are as follows: FSE with drive; repetition time 1500 ms, echo time 250 ms, TSE factor 74, field of view 170×150 mm, slice thickness 0.75 mm, 50 slices, matrix size 512×256, scan time 4 min and 32 s. DRIVE can be used as a sequence in which the driven equilibrium pulse, reset pulse, is applied at the TSE echo train to accelerate relaxation time and return to the equilibrium of Mz magnetization. MRI scan images were reviewed by a paging method on the image monitor retrospectively by at least two experienced radiologists. Black and white reversed images were also adapted for obtaining more contrast between the seventh and eighth nerves and vessels. In addition to ruling out the acoustic schwannoma in the CPA, cerebral vascular disease in the brain stem or cerebellum was also assessed precisely. In practice, flair images are also used for more precise diagnosis. For 14 subjects suspected with insufficient perfusion of vertebrobasilar artery or transient ischemic

attack (TIA)/cerebrovascular disease, plain magnetic resonance angiography (MRA) was performed. In three patients with known aneurysms, computed tomographic angiography (CTA) was also done. The MIP 3D images were used for the evaluation of the vessels in the cerebellopontine cistern.

The distinguishable AICA/PICA branching patterns in CPA area were classified with regard to the existence of loop formation and the IAC extension (see Schema).

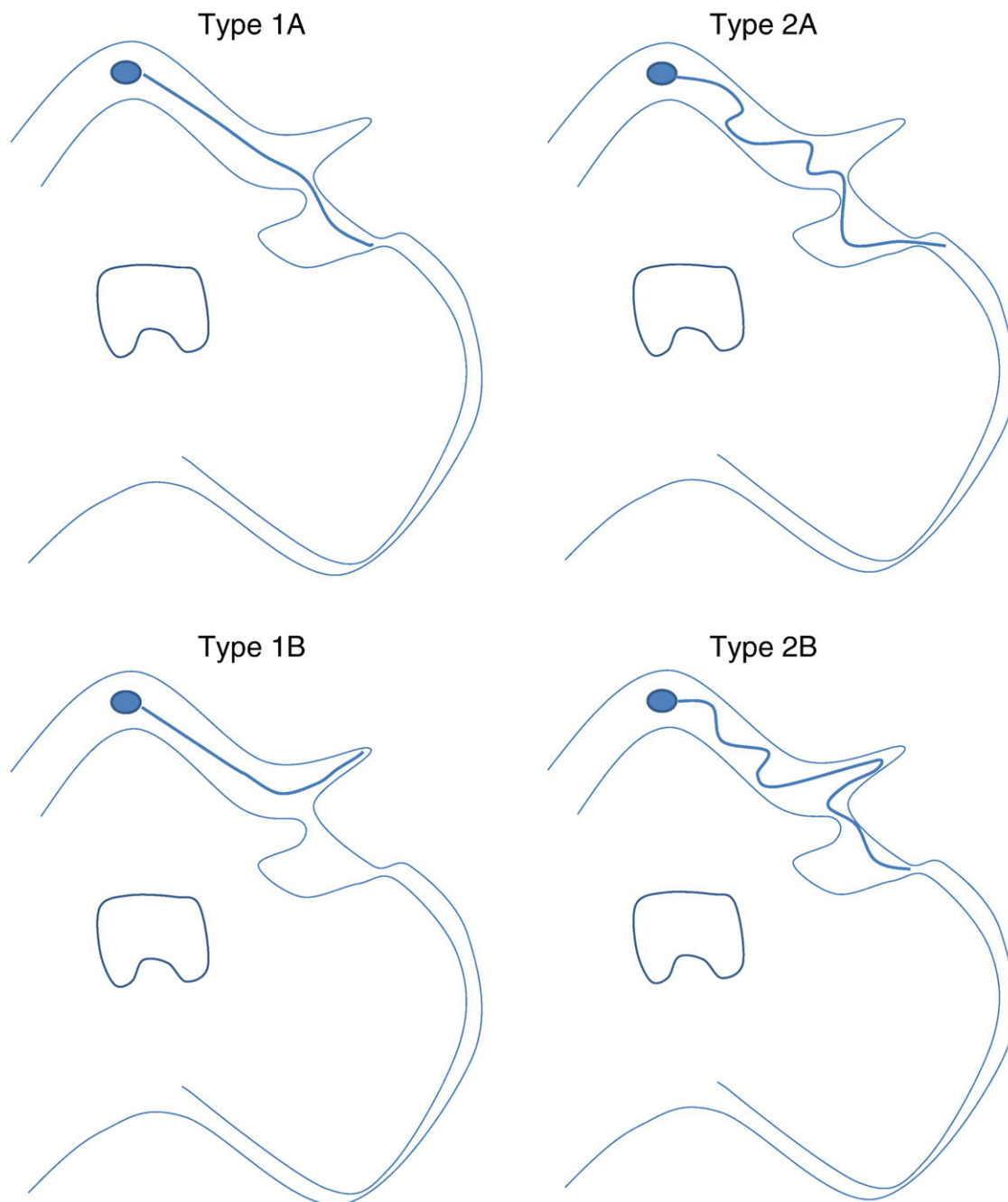
When the distal AICA/PICA crosses the seventh and eighth nerves on at least two slices of axial images, we judged that they contacted with each other. χ^2 test was used for the statistical analysis between the auditory 3 major symptoms and the AICA/PICA running patterns with/without nerve vascular contact.

2. Results

In this study, three acoustic schwannomas (size ranging from 3 mm to 28×25×24 mm) were detected in the IAC or CPA cistern in three patients. Cochlear abnormality such as bilateral hypoplastic anomaly of the inner ear was observed in a 60-year-old female patient with deafness. The dilatation of vestibular aqueduct was also seen in a hearing loss case (Fig. 1). The brain stem lacuna infarction and chronic ischemic foci were observed in two and one case(s), respectively. We also encountered the cerebellar metastatic tumor of 1 cm in diameter with perifocal edema and a cerebellar multilocular cystic lesion (Fig. 2), which was considered to be a perivascular space dilatation or old cerebral lacunar infarct (Fig. 2). In the CPA area, vascular variations, such as the AICA/PICA loop formation, direct extension to the IAC (Figs. 2, 3), and the IAA entering the IAC with branching ($n=3$, 3 sides) (Fig. 4) were observed in this study. The summary of the relationship between the AICA/PICA courses in the CPA area and clinical symptoms is shown in Table 1. The AICA/PICA vascular variations, such as loop formation ($n=33$, 49 sides), direct extension to the IAC ($n=20$, 30 sides), and nerve vascular contact ($n=19$, 27 sides) were revealed.

There were significant differences between type 1A and 2A patients numbers ($P=0.0073<0.01$) regarding the existence of any auditory 3 symptoms (Table 2).

One hundred and eleven AICAs/PICAs from a total of 60 patients were grouped as follows: type 1A ($n=34$, 52 sides), type 1B ($n=6$, 10 sides), type 2A ($n=19$, 29 sides), type 2B ($n=14$, 20 sides), others (aplasia $n=4$). Loop formation was observed in 33 (55%) subjects with 49 ears (Fig. 3). The loop usually forms a laterally convex loop towards or through the meatus. In some cases, differentiation from the adjacent vessels (e.g., pontine, pontine transverse, pontomedullary sulci vein, or basilar venous plexus) in the CPA cistern was difficult. The most common form of the branching patterns was the type 1A, which is a nonloop type outside the IAC orifice and constitutes 56.6%. Types 2A and 2B were relatively frequently seen in 31.7% and 23.3%, respectively.



Schema. Drawing schemas of the AICA/PICA course and shape variations. Type 1A nonloop, AICA/PICA in the CPA cistern (between REZ of the vestibular nerve and the IAC orifice); type 1B, nonloop AICA/PICA (IAA) entering into the IAC; type 2A, loop-type AICA/PICA in the CPA cistern (between REZ of the vestibular nerve and the IAC orifice); and type 2B, loop-type AICA/PICA entering the IAC.

158 There were significant differences between types 1A and 2A
 159 ($P=.012<.05$) with regard to the vertigo. As for the hearing
 160 loss, there were significant differences between types 1A and
 161 2A ($P=.028<.05$) and between types 1A and 2B
 162 ($P=.007<.01$). As for the tinnitus, significant differences
 163 were observed between types 1A and 1B ($P=.0008<.01$) and
 164 between types 1A and 2A ($P=.003<.01$).

165 Contact of the AICA/PICA and vestibulocochlear
 166 nerve was seen in 32.7% of subjects ($n=18, 26$ sides) with
 167 auditory symptoms. Only one artery of a patient (type 2b AICA loop

168 extending to the IAC) contacted with vestibulocochlear
 169 nerve among the five patients with no auditory symptoms.
 170 However, there were no significant differences between the
 171 subgroups regarding the existence of any three symptoms.

3. Discussion

172
 173 MRI including an enhanced study with Gd-DTPA has
 174 been used commonly to rule out the acoustic tumor or

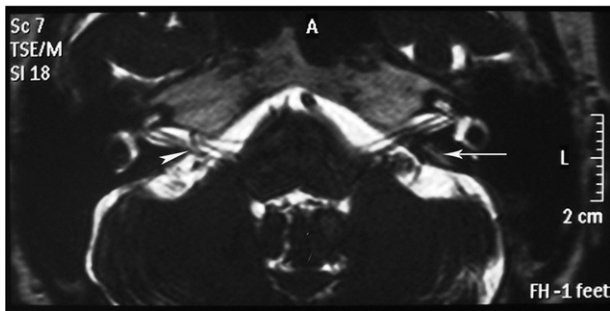


Fig. 1. The dilatation of left vestibular aqueduct (arrow) and an AICA loop formation (arrowheads) in the right IAC of a 68-year-old woman complaining of vertigo were clearly observed on 3D drive T2-weighted MRI.

175 other active inflammatory lesions such as Ramsay–Hunt
 176 syndrome or labyrinthitis in patients with auditory
 177 symptoms. Especially in patients with sensory neural
 178 hearing loss, MRI is superior to computed tomography
 179 in evaluating the inner ear, blood vessels, adjacent fatty
 180 bone marrow, and cerebrospinal fluid (CSF) spaces
 181 because of its superior characterization of soft tissue.
 182 MRI is also useful for the cochlear implantation planning.
 183 For better visualization of the inner ear, heavily T2-
 184 weighted fast spin echo sequences were developed in 1996
 185 [9]. Then, gradient-echo thin-slice sequence such as
 186 constructive interference in steady state (CISS) or balanced
 187 fast field echo image has been introduced widely [10,11].
 188 Three-dimensional CISS is helpful in visualizing faint
 189 structural elements in the central nervous system because

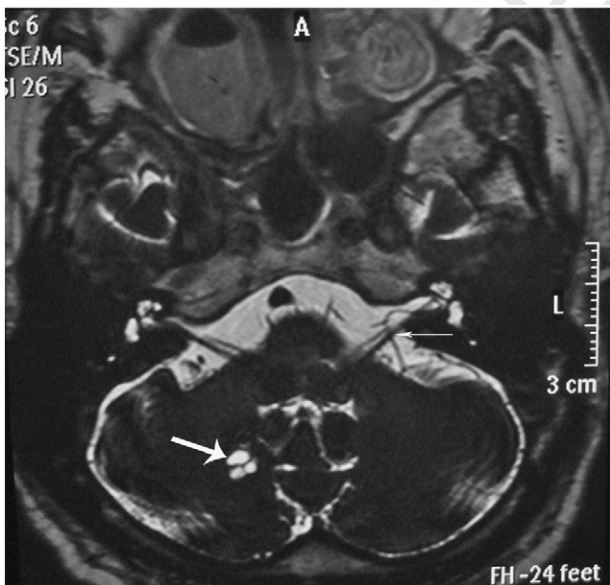


Fig. 2. The cerebellar multilocular cystic lesion (68-year-old man with vertigo) was revealed in the right cerebellar parenchyma adjacent to the vermis (arrowheads) on the 3D drive T2-weighted MRI. We consider it as a variant of perivascular space dilatation, old lacuna infarction, or cavitory degeneration. On the left side, the IAA originated from the ipsilateral AICA and coursed into the left IAC on 3D drive T2-weighted MRI (type IB non-loop-type AICA/PICA without IAC extension).

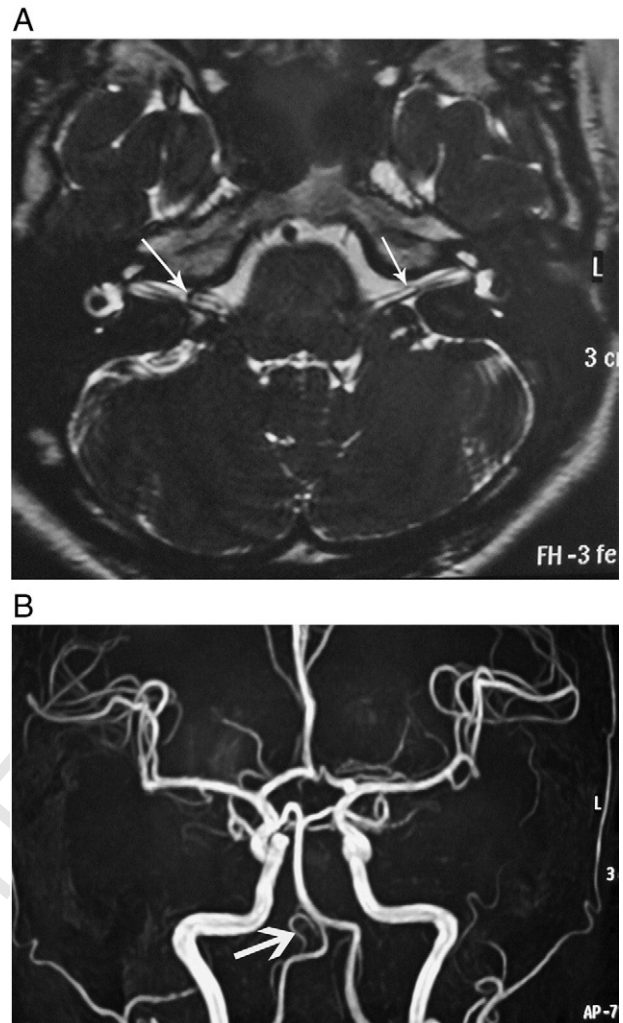


Fig. 3. (A) Bilateral IAAs were observed on high-resolution thin-slice 3D T2-weighted MRI using driven equilibrium pulse sequence. Type IIB loop-type AICA/PICA entering into the IAC with contact to the vestibular nerve (large arrow). We also observed a type IB nonloop AICA/PICA entering into the left IAC (arrow) in a 40-year-old woman with right-sided hearing loss, occasional dizziness, and tinnitus. (B) The right loop-type AICA entering into the IAC was clearly observed on MRA obtained with 0.8-mm thin-slice original images.

of its higher spatial resolution and fewer artifacts from the
 CSF. Recently, the addition of the DRIVE pulse to 3D
 FSE technique, which shortens the scan time and is less
 sensitive to susceptibility artifact, has been introduced.
 Ciftci et al. concluded that the addition of the DRIVE
 pulse to the T2-weighted 3D TSE sequence is preferable
 when imaging the cranial nerves surrounded by the CSF or
 fluid-filled structures because of shorter scan time and
 better image quality due to reduced flow artifacts [12].

The various causes of vertigo (dizziness) or tinnitus are
 enumerated in Tables 3 and 4, respectively. We also have to
 consider not only the auditory organic lesions such as
 acoustic tumor or inner ear inflammatory lesion, but also the
 various CNS diseases, especially cerebellar and brain stem
 diseases [13].

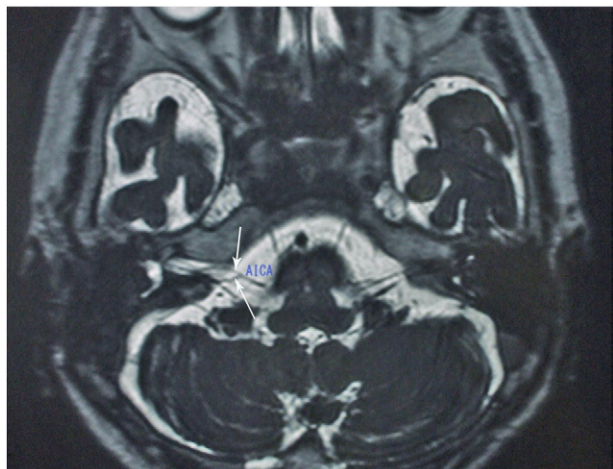


Fig. 4. On 3D drive T2-weighted MRI, we can see the right IAA entering into the IAC with branching (type IB). We can see the bifurcated IAA in a 72-year-old woman with tinnitus (long white arrows).

There were many reports regarding the vascular contact at the root exit zone (REZ) of the facial, trigeminal, and glossopharyngeal nerves which cause hemifacial spasm, trigeminal neuralgia, and glossopharyngeal neuralgia, respectively [8,14–17]. Especially, the supraolivary fossate at the pontomedullary transition area is thought to be the point of the neurovascular compression etiology.

A vascular loop compressing the auditory nerve has been implicated in the etiology of vertigo or tinnitus [18–20]. It is hypothesized that the auditory nerve experiences an “irritation” from a vessel that is in close contact with it. The vertebral artery or basilar artery, superior cerebral artery other than AICA/PICA, or petrosal vein was also recognized as cause for several nerve–vascular compression syndromes [21]. Actually, according to these reports, the compression of the vestibulocochlear nerve caused the gliosis, edema, demyelination, and eventually fibrotic change induced by the axonal degeneration [14,22]. Brain stem auditory nuclei may be secondarily affected by changes in the auditory nerve and be the actual generator site(s) for the tinnitus. Our study can also reveal the possibility of nerve vascular compression syndrome for the vertigo, sensory hearing loss, and tinnitus especially in the group of types 1B (nonloop type with IAC extension) and 2B (loop type with IAC extension). Although 55 patients had symptoms potentially related to vestibular or cochlear nerve dysfunction, it is difficult to know to what degree AICA contact with nerves had attributed to

Table 1
The relationships of the AICA/PICA branching/coursing patterns and three major auditory symptoms

Type (pattern)	Vertigo	Hearing loss	Tinnitus	None
1A (B18 U16 52s)	10	3	2	4
B (B4 U2 10s)	2	2	3	1
2A (B10 U9 29s)	13	7	7	1
B (B6 U8 20s)	7	6	4	1

B, bilateral; U, unilateral; s, side.

Table 2
Summary of the AICA/PICA subtype patients' numbers and the presence of any symptoms

Symptom	No symptom	Total
1A	12	22
1B $P=.0073$	3	3
2A	14	5
2B	8	6

vestibulocochlear nerve function mainly because of the resolution of MR images. Conversely, clearly visualized IAA (AICA/PICA extension to the IAC) means the luminal dilatation of the artery caused by the hypertensive atherosclerosis or angitic changes. Then it is not unnatural for these vessels to evoke the auditory symptoms.

Of course, in five subjects without the major three auditory symptoms, we performed this 3D drive thin-slice T2WI MRI. In one of them, we observed the 2b type AICA loop extending to the IAC; however, we think that these exceptional cases have a potential risk of eliciting any auditory symptoms even if normal in their life. Gorrie et al. identified AICA loop running between the facial and the vestibulocochlear nerve, and some loops were displacing the vestibulocochlear nerve. In these cases, further investigation was deserved, although no significant association was found between the other type of AICA loop and the vestibulocochlear nerve [23].

MRI using sense coil with drive pulse can display relatively high-quality image because of less susceptibility to artifact than balanced FFE T2 gradient images. However, images of 3D drive T2WI have little less contrast between the cerebral gray and white matter. So careful observation is necessary for excluding the tiny ischemic or demyelinating lesions in the brain stem and the cerebellar parenchyma. In practice, flair images or diffusion-weighted images are also used for more precise diagnosis. Concerning the diagnosis of the inner ear structural disorder such as Mondini-type anomaly which is the most common type of dysplastic

Table 3
The causes of vertigo [1–3,5,6]

Peripheral (approximately 70%) origin	
Meniere's disease	
Sudden sensorineural hearing loss with vertigo	
Vestibular neuritis (labyrinthitis)	
Benign paroxysmal positional vertigo	
Acoustic tumor	
Inner ear infection	
Drug (aminoglycosides, streptomycin and gentamicin)	
Ramsay Hunt syndrome	
Trauma (e.g., perilymphatic fistula)	
Central origin (20%)	
Brain or cerebellar lesion (infarction, hemorrhage, tumor)	
Vertebrobasilar perfusion insufficiency	
TIA	
Cerebellar degeneration syndromes	
Multiple sclerosis	
Others (10%): psychogenic dizziness, hypertension, hypotension, arrhythmia	

t4.1	Table 4
t4.2	The causes of tinnitus
t4.3	Peripheral origin
t4.4	Meniere's disease
t4.5	Sudden sensorineural hearing loss
t4.6	Vestibular neuritis (labyrinthitis)
t4.7	Acoustic tumor
t4.8	Inner ear infection
t4.9	Otitis media
t4.10	Drug (aminoglycosides, salicylates, heavy metal, alcohol, and diuretics)
t4.11	Ramsay Hunt syndrome
t4.12	Trauma (tympanic membrane injury)
t4.13	External ear lesion
t4.14	Central origin
t4.15	Brain or cerebellar lesion (infarction, hemorrhage, tumor)
t4.16	Vertebrobasilar perfusion insufficiency
t4.17	Arachnoiditis
t4.18	Others: hypertension, hypothyroidism, anemia.

anomaly, or dilatation of vestibular aqueduct, heavily T2-weighted 3D drive images are very useful [23]. Its sequence would be expected to be very useful for the preservation of the IAA at surgical therapy or the preoperative planning for the artificial inner ear device. Of course, the knowledge of the AICA/PICA course and branching patterns revealed by this study would be useful for the operation not only to decide the appropriate decompression site but also to avoid vascular injury leading to massive hemorrhage. However, because of the spatial resolution (the voxel size was 0.33 mm×0.59 mm×0.75 mm in most subjects), microstructure less than about 0.5mm in diameter such as distal IAA (labyrinthine artery), cochlear aqueduct have not been fully visualized yet.

The limitation of our study is that the three-dimensionally coursing pattern should be confirmed by not only the thin-slice CTA but also the digital subtraction angiography in order to make the precise assessment of the origin of CPA vessels because the IAA did not always originate from AICA/PICA but sometimes arise directly from basilar artery with asymmetric branching patterns. However, our paging cine-like image review method of thin-slice MRI with MRA can evaluate the relationship between the distal branch of the AICA/PICA and VIIth–VIIIth nerves to some extent. Further study using higher-resolution image including coronal image or 3D displays on more subjects would be necessary to elucidate what degree of AICA contacting with vestibulocochlear nerves had attributed to nerve dysfunction. The other factor affecting the nerve is a postural physical effect, such as mechanical load during the flexion and extension movements of the head and neck [24].

In conclusion, on high-resolution ultra-thin-slice 3D T2-weighted MRI using driven equilibrium pulse sequences, we were able to detect inner auditory canal tumor of 3 mm in size without contrast material. The cochlear hypoplastic anomaly was also observed clearly. The AICA/PICA branching and configuration patterns relative to the IAC were classified into four major types with special reference to the loop formation and the IAC extension. The nerve

vascular contact was observed in 18 (32.7%) cases. There was a significant association between the group of the IAC extension of AICA/PICA and the auditory symptoms. Therefore, we believe that this classification is simple and very useful for deciding the surgical therapeutic strategies and for the elucidation of the pathophysiology of the major auditory symptoms regarding the anatomical relationship of the nerve and vessels.

References

- [1] Daniels DL, Herfkens R, Koehler PR, et al. Magnetic resonance imaging of the internal auditory canal. *Radiology* 1984;151:105–8.
- [2] Schmalbrock P, Chakersres DW, Monroe JW, et al. Assessment of internal auditory canal tumors :a comparison of contrast-enhanced T1-weighted and steady-state T2-weighted gradient-echo MR imaging. *Am J Neuroradiol* 1999;20:1207–13.
- [3] Rinaldo FC, Paul RL. Tinnitus. *The ear: comprehensive otology*. LWW, 2000. p. 565.
- [4] Lunsford LD, Niranjan A, Flickinger JC, et al. Radiosurgery of vestibular schwannomas: summary of experience in 829 cases. *J Neurosurg* 2005;102(Suppl):195–9.
- [5] Amarenco P, Rosenqart A, Dewitt LD, et al. Anterior inferior cerebellar artery territory infarcts. Mechanism and clinical features. *Arch Neurol* 1993;50:154–61.
- [6] Kumral E, Kisabav A, Atac C. Lesion pattern and etiology of ischemia in the anterior inferior cerebellar artery territory involvement: a clinical-diffusion weighted-MRI study. *Eur J Neurol* 2006;13:395–401.
- [7] Murakami T, Nakayasu H, Doi M, et al. Anterior and posterior inferior cerebellar artery infarction with sudden deafness and vertigo. *J Clin Neurosci* 2006;13:1051–4.
- [8] Moller MB, Moller AR, Jennetaa PJ. Vascular decompression surgery for severe tinnitus :selection criteria and results. *Laryngoscope* 1993;103:421–7.
- [9] Naganawa S, Yamakawa K, Fukatsu H, et al. High-resolution T2-weighted MR imaging of the inner ear using a long echo-train-length 3D fast spin echo sequence. *Eur Radiol* 1996;06:369–74.
- [10] Stuckey SL, Harris AJ, Mannolini SM. Detection of acoustic schwannoma: use of constructive interference in the steady state three-dimensional MR. *AJNR Am J Neuroradiol* 1996;17:1219–25.
- [11] Czerny C, Rand T, Gstoettner W, et al. MR imaging of the inner ear and cerebellopontine angle: comparison of three-dimensional and two-dimensional sequences. *AJR Am J Roentgenol* 1998;170:791–6.
- [12] Ciftci E, Anik Y, Arslan A, et al. Driven equilibrium (drive) MR imaging of the cranial nerves V–VIII: comparison with the T2-weighted 3D TSE sequence. *Eur J Radiol* 2004;51:234–40.
- [13] Cawthorne T. Meniere's disease. *Ann Otol Rhinol Laryngol* 1957;56:18–38.
- [14] Wilkins RH. Neurovascular compression syndromes. *Neurol Clin* 1985;3:359–72.
- [15] Adams CB. Microvascular compression: an alternative view and hypothesis. *J Neurosurg* 1989;70:1–12.
- [16] Sindou M, Leston J, Decullier E, et al. Microvascular decompression for primary trigeminal neuralgia: long-term effectiveness and prognostic factors in a series of 362 consecutive patients with clear-cut neurovascular conflicts who underwent pure decompression. *J Neurosurg* 2007;107:1144–53.
- [17] Naragshi R, Tanrikulu L, Troescher WR, et al. Classification of neurovascular compression in typical hemifacial spasm: three-dimensional visualization of the facial and the vestibulocochlear nerves. *J Neurosurg* 2007;107:1154–63.
- [18] Mailer MB. Results of microvascular decompression of the eighth nerve as a treatment for disabling positional vertigo. *Ann Otol Rhinol Laryngol* 1990;99:724–9.

- 363 [19] Makins AE, Nikolopoulos TP, Ludman C. Is there a correlation
364 between vascular loops and unilateral auditory symptoms? *Laryngo-*
365 *scope* 1998;108:1739–42.
- 366 [20] Schwaber MK, Whthshell WO. Cochleovestibular nerve compression
367 syndrome. 2 vestibular nerve histopathology and theory of pathophys-
368 iology. *Laryngoscope* 1992;102:1030–6.
- 369 [21] Fukuda H, Ishikawa M, Okumura R. Demonstration of neurovascular
370 compression in trigeminal neuralgia and hemifacial spasm with
371 magnetic resonance imaging comparison with surgical findings in 60
372 consecutive cases. *Surg Neurol* 2003;59:93–9.
- [22] Jung NY, Moon WJ, Lee MH, Chung EC. Magnetic resonance 373
cisternography: comparison between 3-dimensional driven equilibrium 374
with sensitivity encoding and 3-dimensional balanced fast-field echo 375
sequences with sensitivity encoding. *J Comput Assist Tomogr* 2007; 376
31:588–91. 377
- [23] Gorrie A, Warren FM, de la Garza AN, et al. Is there a correlation 378
between vascular loops in the cerebellopontine angle and unexplained 379
unilateral hearing loss? *Otol Neurotol* 2010;31(1):48–52. 380
- [24] Rossitti S. Biomechanics of the pons-cord tract and its enveloping 381
structures: an overview. *Acta Neurochir (Wien)* 1993;124:144–52. 382
383

UNCORRECTED PROOF

AUTHOR QUERY FORM

 ELSEVIER	Journal: JCT Article Number: 7155	Please e-mail or fax your responses and any corrections to: Nina Biuso E-mail: nbiuso@aol.com Tel: 845-896-0870 Fax: 845-896-0870
--	--	--

Dear Author,

Please check your proof carefully and mark all corrections at the appropriate place in the proof (e.g., by using on-screen annotation in the PDF file) or compile them in a separate list. Note: if you opt to annotate the file with software other than Adobe Reader then please also highlight the appropriate place in the PDF file. To ensure fast publication of your paper please return your corrections within 48 hours.

For correction or revision of any artwork, please consult <http://www.elsevier.com/artworkinstructions>.

Any queries or remarks that have arisen during the processing of your manuscript are listed below and highlighted by flags in the proof. Click on the 'Q' link to go to the location in the proof.

Location in article	Query / Remark: click on the Q link to go Please insert your reply or correction at the corresponding line in the proof
Q1	Please confirm that given names and surnames have been identified correctly.
Q2	Please check this for clarity.
Q3	Please check if the keywords were captured correctly.
Q4	Please check if this should be changed to "At the same time" or "Sometimes."
Q5	Please define at first use.
Q6	Please check data here.
Q7	Please define at first use if an abbreviation/acronym.
Q8	Please spell out.
Q9	Text was rephrase and citation of schema was inserted here, please check if we may proceed. Thank you.
Q10	Please check this for clarity.
Q11	Please clarify what a "Type" is? Is this a figure? If yes, Type means "the patterns of artery course and figure", So type 3 (AICA?PICA aplasia or hemiplasia) should be deleted. It corrected as "others" in text. Please check if appropriate.
Q12	Please spell out.
Q13	Please spell out.
Q14	Use of the plural verb here implies that it refers to "nerves" and not "vascular contact" or "root exit zone." Please advise if this is indeed the case.
Q15	Please check word used here.

Q16	Please spell out.
Q17	Please check this sentence for clarity.
Q18	Please provide publisher location.

Thank you for your assistance.